

Establishment and application of flow stress models of Mg-Y-MM-Zr alloy

MA Ming-long¹, LI Xing-gang¹, LI Yong-jun¹, HE Lan-qiang¹, ZHANG Kui¹, WANG Xian-wen², CHEN Li-fang²

1. State Key Laboratory of Non-ferrous Metals and Processes, Beijing General Research Institute for Non-ferrous Metals, Beijing 100088, China;
2. Southwest Aluminum (Group) Co., Ltd, Chongqing 401326, China

Received 25 September 2010; accepted 25 December 2010

Abstract: The hot working behaviors of Mg-9Y-1MM-0.6Zr (WE91) magnesium alloy were researched in a temperature range of 653–773 K and strain rate range of $0.001-1 \text{ s}^{-1}$ on Gleeble-1500D hot simulator under the maximum deformation degree of 60%. A mathematical model was established to predict the stress–strain curves of this alloy during deformation. The experimental results show that the relationship between stress and strain is obviously affected by the strain rates and deformation temperatures. The flow stress of WE91 magnesium alloy during high temperature deformation can be represented by Zener-Hollomon parameter in the hyperbolic Arrhenius-type equation, and the stress–strain curves obtained by the established model are in good agreement with the experimental results, which prove that the model reflects the real deformation characteristics of the WE91 alloy. The average deformation activation energy is 220 kJ/mol at strain of 0.1. The microstructures of WE91 during deformation processing are influenced by temperature and strain rates.

Key words: rare-earth magnesium alloy; Zener-Hollomon parameter; flow stress model; microstructure

1 Introduction

Because of the low densities and excellent properties, such as heat dissipation, damping, electromagnetic shielding and recycling, the structure applications of magnesium alloys in aerospace and automobile industries are increasing progressively[1–2]. Compared with as-cast magnesium alloys, wrought magnesium alloys possess greater potential due to higher strength, better plasticity and various mechanical properties. Magnesium alloys have poor plastic deformation property because of the hexagonal close-packed structure and low stacking fault energy[3–4]. Addition of rare earth elements could remarkably improve grain refinement, heat resistant capacity and high temperature properties, so magnesium alloys with rare earth elements have much more attractiveness than others[5–6]. Magnesium alloys containing rare earth elements Gd and/or Y have been developed and extensively investigated recently such as Mg-8Gd-0.6Zr-xNd-yY($x+y=3$), Mg-11Gd-2Nd-0.5Zr and Mg-10Gd-3Y-1.2Zn-0.4Zr[7–9]. However, the works on the deformation behaviors of Mg-Y-MM-Zr are

quite limited. Therefore, the aim of the present investigation is to study the hot deformation behaviors, establish and apply a flow stress model of a sort of rare-earth magnesium alloy, so as to provide both a theoretical and an experimental background for calculation of mechanical parameters and the technique process optimization of magnesium alloy in plastic deformation.

2 Experimental

The chemical composition (mass fraction, %) of the alloy used in this investigation was as follows: Y 9.06, MM (MM: La30, Ce48, Nd18, Pr3) 1.07, Zr 0.42, and balance Mg (WE91). The test alloy was homogenized at 803–808 K for 18 h and water quenched with the microstructure shown in Fig.1, which consisted of intermetallic compounds of Mg-MM and Mg-Y at the grain boundaries. Cylindrical specimens for the compression tests were machined to 10 mm in diameter and 15 mm in height. Thin graphite sheets were placed between the compression specimen and the die during the test in order to decrease the friction and maintain uniform deformation. Isothermal hot compression tests

were carried out on a Gleeble–1500D thermal mechanical simulator in the temperature range of 653–773K and at a constant strain rate in the range of $0.001\text{--}1\text{ s}^{-1}$. The specimens were heated to the deformation temperature at 5 K/s, where holding time of heat preservation was 2 min. The specimens were deformed up to a true strain of about 0.916. The specimen was water quenched in order to keep the microstructure at a high temperature as soon as the deformation was completed.

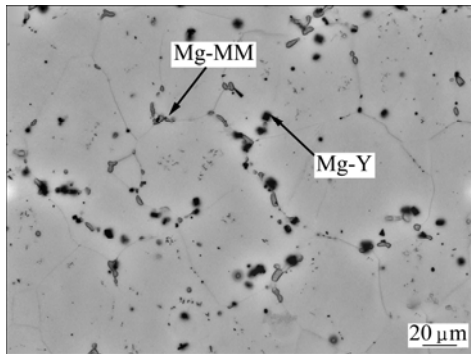


Fig.1 Microstructure of WE91 alloy after homogenization at 803–808 K for 18 h

3 Results and discussion

3.1 True stress—strain curves

The typical true stress—true strain curves of WE91 magnesium alloy at different deformation temperatures and various strain rates are presented in Fig.2, which reflect the influence of temperature, strain rate on strain flow stress. From Fig.2, it can be seen that all curves exhibit a sharp increase at initial deformation stage of strain followed by steady state flow. Otherwise, flow stress decreases with decreasing strain rate (Fig.2(a)) and increases with decreasing temperature (Fig.2(b)). Most of the flow stress curves consist of four stages: work hardening, transition, softening and steady state, which means that both work hardening and thermally activated softening mechanisms play important roles in the plastic deformation[10]. Consequently, WE91 alloy belongs to a material with positive strain rate sensitivity.

3.2 Flow stress model

Hot deformation is a process of thermal activation; therefore, it obeys the Arrhenius equation which is used to describe the relationship between the strain rates especially at high temperature[11]. ZENER and HOLLomon proposed that a material flow stress model could be expressed as a function of strain, strain rate and temperature, and the relationship of temperature and strain rate could be also denoted by a parameter Z , the physical meaning of which is the so-called temperature compensated strain rate parameter[12–13]:

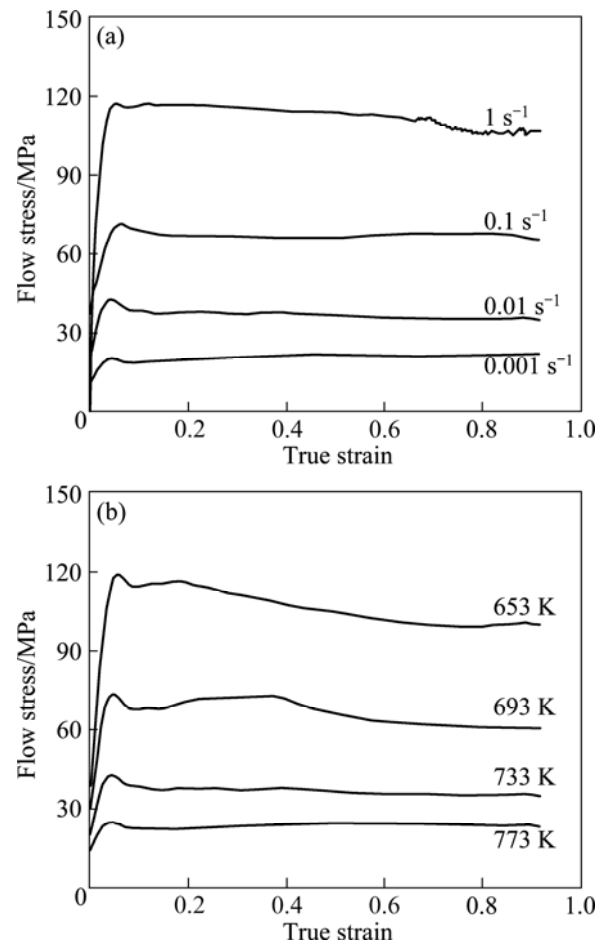


Fig.2 True stress—strain curves of WE91 alloy at different conditions: (a) 733 K; (b) $\dot{\epsilon}=0.01\text{ s}^{-1}$

$$\sigma = \sigma(Z, \epsilon) \quad (1)$$

$$Z = \dot{\epsilon} \exp[Q/(RT)] \quad (2)$$

where σ is the flow stress; Q is the average apparent activation energy of deformation; $\dot{\epsilon}$ is the strain rate; R is the ideal gas constant; Z is Zener-Hollomon parameter; T is the deformation temperature.

Commonly, the relationship between the strain rate and flow stress conforms to the following equations[13]:

$$\dot{\epsilon} = A_1 \sigma^n \quad (3)$$

$$\dot{\epsilon} = A_2 \exp(\beta\sigma) \quad (4)$$

$$\dot{\epsilon} = A[\sinh(\alpha\sigma)]^n \exp[-Q/(RT)] \quad (5)$$

where n_1 , n , A_1 , A_2 , A , β , and α ($\alpha = \beta/n_1$) are material constants. Eq.(3) and Eq.(4) are commonly applied to low stress and high stress, respectively. Eq.(5) is generally used to describe the flow stress and deformation activation behavior over a wide range of temperatures and strain rates, which is in the hyperbolic sine law proposed by SELLARS and TEGART. Therefore, a constitutive equation for WE91 alloy is proposed by

employing hyperbolic-sine-type equation.

Because the value of α is independent of the temperatures and strain levels[14–15], it can be easily obtained. The hot deformation activation energy, which is an important physical parameter serving as indicator of deformation difficulty degree with plasticity deformation, theory can be calculated with the following equation:

$$Q = R \left\{ \frac{\partial \ln \dot{\epsilon}}{\partial \ln[\sinh(\alpha\sigma)]} \right\}_T \left\{ \frac{\partial \ln[\sinh(\alpha\sigma)]}{\partial (1/T)} \right\}_{\dot{\epsilon}} \quad (6)$$

The values of flow stresses at strain of 0.1 were used to establish the model as an example. By linear regression of the relations of $\ln\sigma - \ln\dot{\epsilon}$ (Fig.3(a)) and $\sigma - \ln\dot{\epsilon}$ (Fig.3(b)) at different temperatures, α is determined as 0.015 MPa^{-1} . Figure 3(c) shows the relationship between $\ln[\sinh(\alpha\sigma)]$ and $\ln\dot{\epsilon}$. And Fig.3(d) shows the relationship between $\ln[\sinh(\alpha\sigma)]$ and $1/T$. The average of regression coefficients of several groups of parallel and straight lines is greater than 0.99. The hot deformation activation energy Q of WE91 alloy is determined through substituting the slopes of Fig.3(c) and Fig.3(d) into Eq.(6), and the calculated value is

obtained to be about 220 kJ/mol.

The previous study indicates Q , $\ln A$, n and α have a connection to strain (ϵ)[16–17]. To describe precisely the relation of them, a group of equations can be established as follows:

$$\begin{cases} Z = \dot{\epsilon} \exp\left(\frac{Q}{RT}\right) = A[\sinh(\alpha\sigma)]^n \\ Q = B_0 + B_1\epsilon + B_2\epsilon^2 + B_3\epsilon^3 + B_4\epsilon^4 + B_5\epsilon^5 \\ \ln A = C_0 + C_1\epsilon + C_2\epsilon^2 + C_3\epsilon^3 + C_4\epsilon^4 + C_5\epsilon^5 \\ n = D_0 + D_1\epsilon + D_2\epsilon^2 + D_3\epsilon^3 + D_4\epsilon^4 + D_5\epsilon^5 \\ \alpha = E_0 + E_1\epsilon + E_2\epsilon^2 + E_3\epsilon^3 + E_4\epsilon^4 + E_5\epsilon^5 \end{cases} \quad (7)$$

where B_x , C_x , D_x and $E_x(x=1, 2, 3, 4, 5)$ are material parameters of the model. $B_0=212$, $B_1=96$, $B_2=107$, $B_3=-1277$, $B_4=2146$, $B_5=-1095$; $C_0=30$, $C_1=38$, $C_2=-62$, $C_3=-71$, $C_4=237$, $C_5=-143$; $D_0=3$, $D_1=-2$, $D_2=20$, $D_3=-55$, $D_4=64$, $D_5=-27$; $E_0=0.018$, $E_1=-0.039$, $E_2=0.10$, $D_3=-0.12$, $D_4=0.063$, $E_5=-0.015$.

It can be found that according to Eq.(7), the model contains only one parameter ϵ , which is taken as a

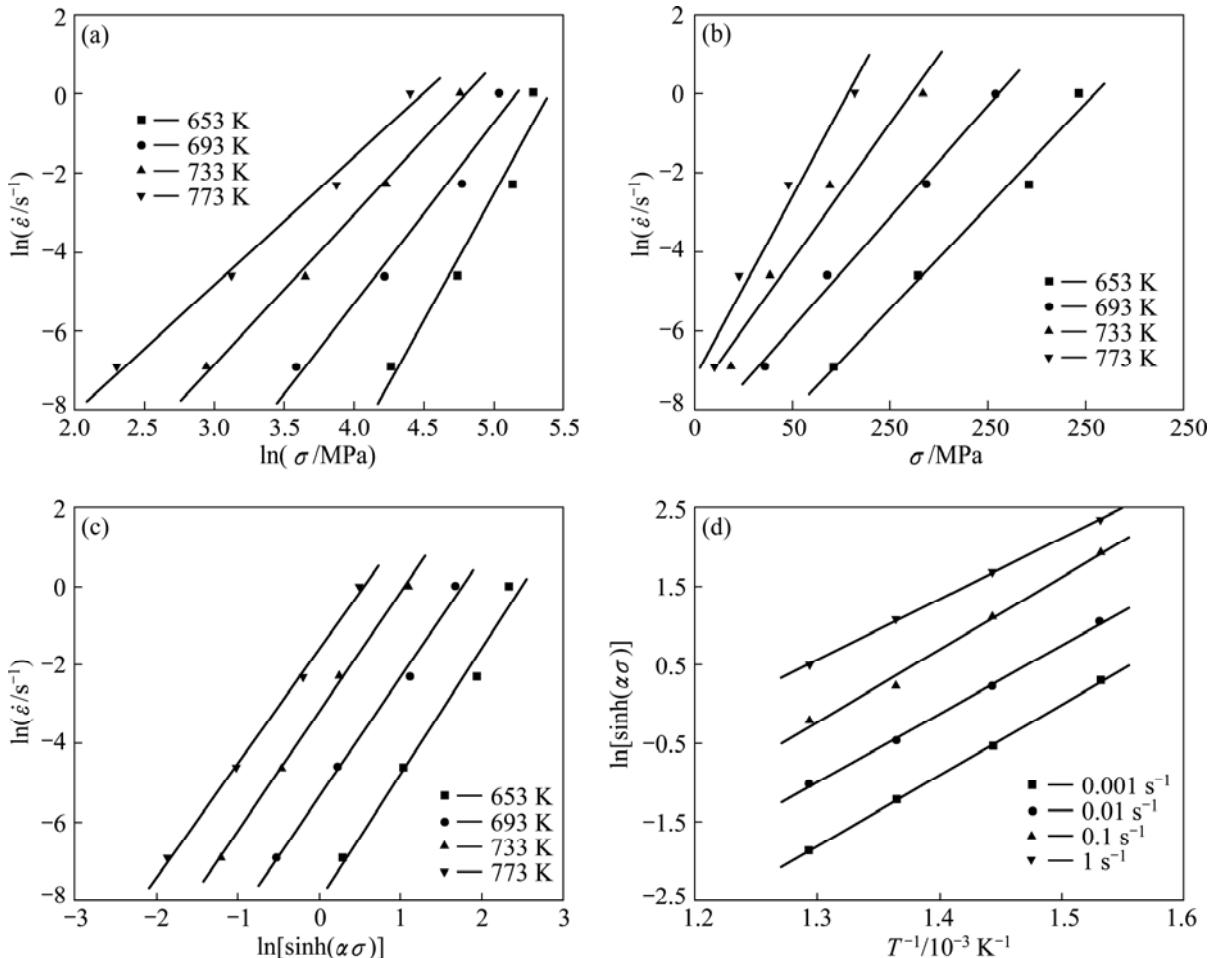


Fig.3 Relationships of peak stress, strain rate and temperature during plastic deformation: (a) $\ln\sigma - \ln\dot{\epsilon}$; (b) $\sigma - \ln\dot{\epsilon}$; (c) $\ln[\sinh(\alpha\sigma)] - \ln\dot{\epsilon}$; (d) $\ln[\sinh(\alpha\sigma)] - T^{-1}$

constant parameter in the beginning of building the model of flow stress. In order to obtain the flow stress, Eq.(5) can be transformed and expressed as

$$\sigma = \frac{1}{\alpha} \operatorname{arcsinh} \left\{ \exp \left[\frac{\ln \dot{\varepsilon} - \ln A + Q/(RT)}{n} \right] \right\} \quad (8)$$

which is relative to Q , $\ln A$, n and α . The values of B_x , C_x , D_x and E_x can be given by regression calculation at various deformation temperatures and strain rates. The relationships of Q , $\ln A$, n , α and strain (ε) are shown in Fig.4. The values of Q , $\ln A$, n and α are taken into Eq.(8); hence, the flow stress can be obtained.

The flow stress curves can be sketched as shown in Fig.5 according to Eq.(8). It is indicated that calculated stresses have a good fitness with experimental ones. By deviation calculation under all the experimental conditions, the total mean square deviation is less than 6.

3.3 Microstructure evolution

The optical microstructures of WE91 magnesium alloy after hot deformation are shown in Fig.6. At the deformation temperature of 693 K (Fig.6(a)), all of the grains are elongated in the perpendicular direction of compression axis and a few small recrystallized grains develop along the initial grain boundaries. The

recrystallized grains can be distinguished when the temperature is higher, as shown in Figs.6(b) and (d). After temperature increases to 773 K, recrystallized grains are seen to grow up obviously.

In addition, strain rate has important effects on the deformation microstructures. The flow softening seems more pronounced at low strain rate which is evident from Figs.6(b) and (c). At high strain rate, dislocations have no enough time to consume since the accumulated energy increases; the density is higher and the recrystallized grains are finer. While the strain rate is relatively lower, DRX grains have more time to nucleate and grow up and dislocations density decreases.

4 Conclusions

1) WE91 alloy belongs to a material with positive strain rate sensitivity. Lower temperature and higher strain rate can increase the flow stress of alloy.

2) A model of flow stress about WE91 is established and the stress predicted by the model matches well with the Gleeble test data and has higher precision.

3) The microstructures of WE91 magnesium alloy during hot deformation are influenced by temperature

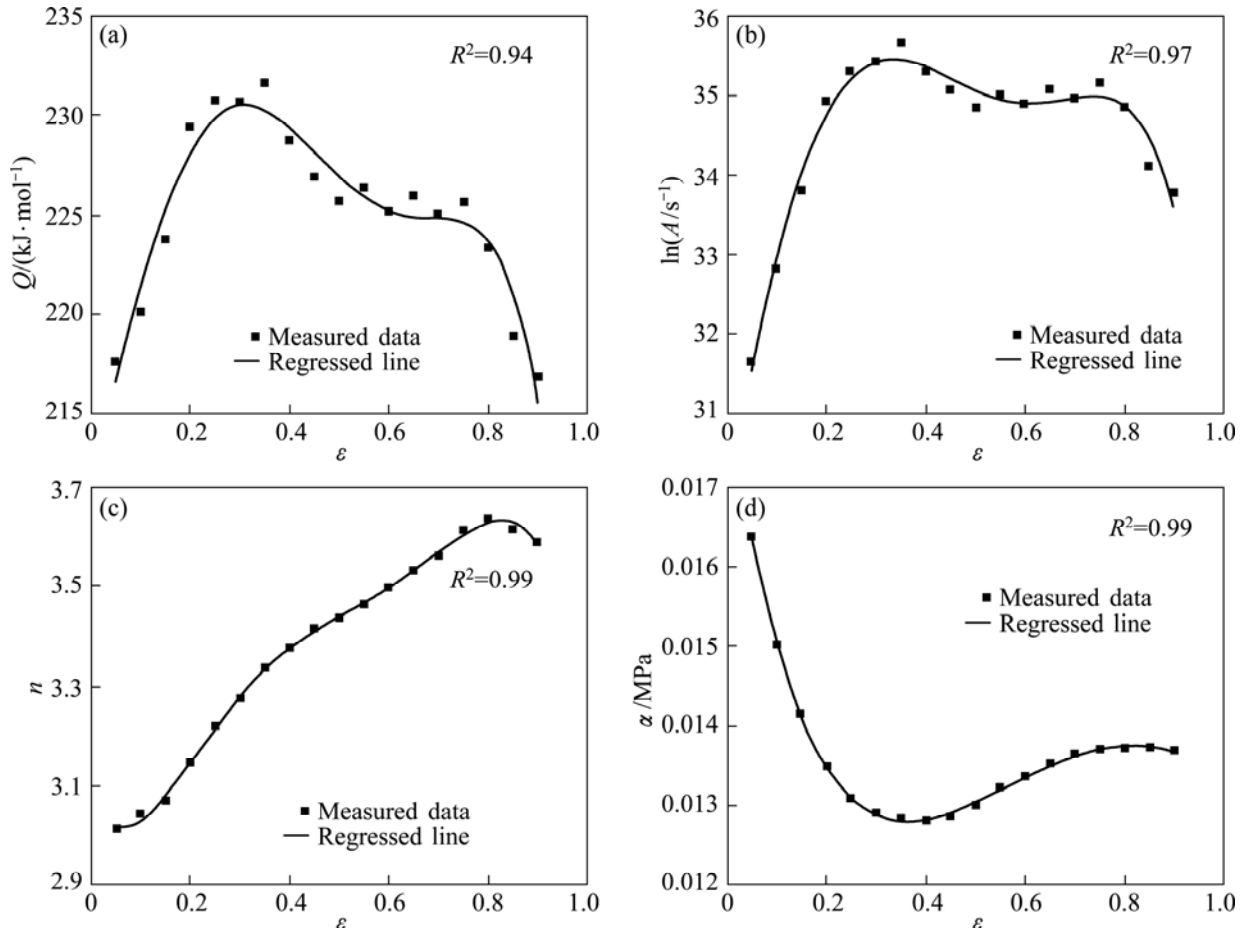


Fig.4 Relationships between material parameter and strain: (a) $Q-\varepsilon$; (b) $\ln A-\varepsilon$; (c) $n-\varepsilon$; (d) $\alpha-\varepsilon$

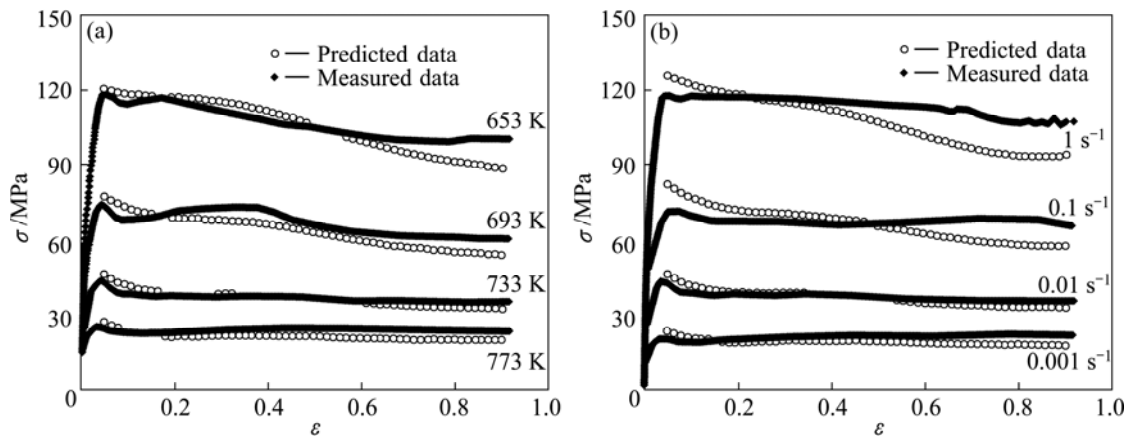


Fig.5 Comparison between model prediction results and experimental results of WE91: (a) $\dot{\varepsilon}=0.01 \text{ s}^{-1}$; (b) $T=733 \text{ K}$

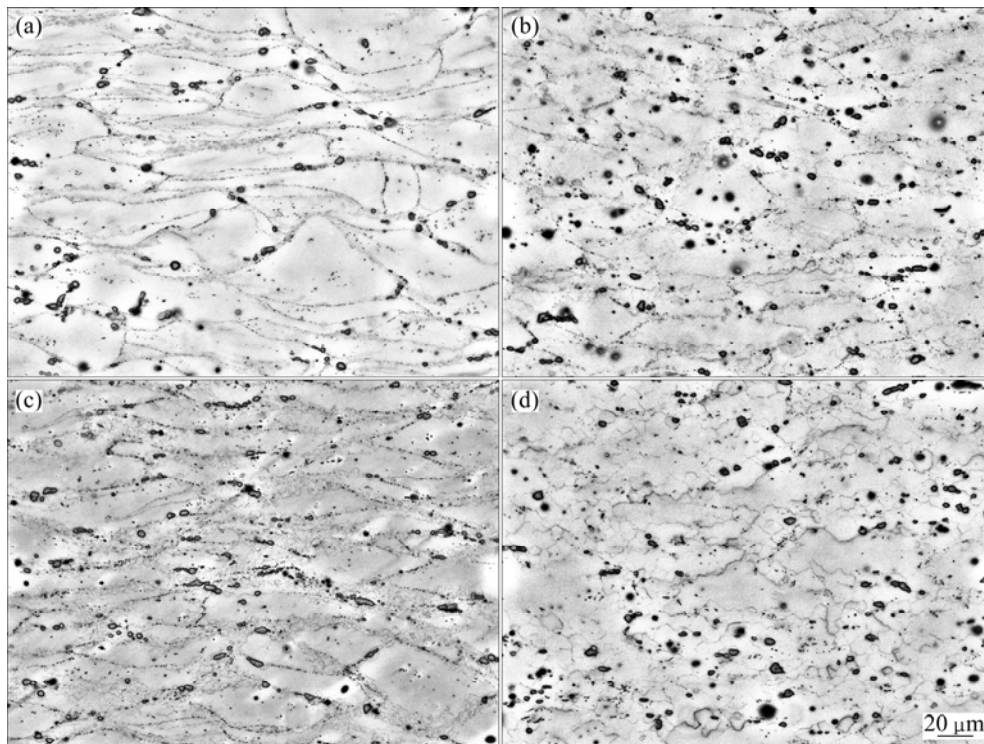


Fig.6 Optical microstructures of WE91 magnesium alloy at different temperatures and strain rates (ε is 0.916): (a) $T=693 \text{ K}$, $\dot{\varepsilon}=0.01 \text{ s}^{-1}$; (b) $T=733 \text{ K}$, $\dot{\varepsilon}=0.01 \text{ s}^{-1}$; (c) $T=733 \text{ K}$, $\dot{\varepsilon}=1 \text{ s}^{-1}$; (d) $T=773 \text{ K}$, $\dot{\varepsilon}=0.01 \text{ s}^{-1}$

and strain rate. Fine recrystallized grains are obtained at higher strain rates and recrystallized grains grow up at higher temperature.

References

- [1] CHANG Jian-wei, GUO Xing-wu, FU Peng-huai, PENG Li-ming, DING Wen-jiang. Effect of heat treatment on corrosion and electrochemical behaviour of Mg-3Nd-0.2Zn-0.4Zr (wt. %) alloy [J]. *Electrochimica Acta*, 2007, 52(9): 3160–3167.
- [2] MORDIKE B L, EBERT T. Magnesium: Properties-applications-potential [J]. *Material Science and Engineering A*, 2001, 302(1): 37–45.
- [3] CAHN R W. Materials science and technology: Structure and properties of nonferrous alloys (Vol.8) [M]. DIANG Dao-yun. Beijing: Science Press. 1999.
- [4] LIU Juan, CUI Zheng-shan, LI Cong-xing. Modeling of flow stress characterizing dynamic recrystallization for magnesium alloy AZ31B [J]. *Computer Materials Science*, 2008, 41(3): 375–382.
- [5] ZHOU H T, ZHANG Z D, LIU C M, WANG Q W. Effect of Nd and Y on the microstructure and mechanical properties of ZK60 [J]. *Material Science and Engineering A*, 2007, 445–446: 1–6.
- [6] ROKLIN L L. Magnesium alloy containing rare-earth metals: Structures and properties [M]. New York: Taylor & Francis, 2002.
- [7] PENG Qiu-ming, WANG Jian-li, WU Yao-ming, WANG Li-min. Microstructures and tensile properties of Mg-8Gd-0.6Zr-xNd-yY ($x+y=3$, mass%) alloys [J]. *Material Science and Engineering A*, 2006, 433(1–2): 133–138.
- [8] ZHENG K Y, DONG J, ZENG X Q, DING W J. Precipitation and its effect on the mechanical properties of a cast Mg-Gd-Nd-Zr alloy [J]. *Material Science and Engineering A*, 2008, 489(1–2): 44–54.

- [9] LI D J, ZENG X Q, DONG J, ZHAI C Q, DING W J. Microstructure evolution of Mg-10Gd-3Y-1.2Zn-0.4Zr alloy during heat-treatment at 773 K [J]. Journal of Alloys and Compounds, 2009, 468(1-2): 164–169.
- [10] LIN Y C, CHEN Ming-song, ZHONG Jue. Prediction of 42CrMo steel flow stress at high temperature and strain rate [J]. Mechanics Research Communications, 2008, 35(3): 142–150.
- [11] GOURDET S, MONTHEILLET F. An experimental study of the deformation of a 304 type austenitic stainless steel [J]. Materials Science and Engineering A, 1998, 255(1-2): 139–147.
- [12] TAKUDA H, FUJIMOTO H, HATTA N. Modeling on flow stress of Mg-Al-Zn alloys at elevated temperatures [J]. Materials Processing Technology, 1998, 80-81: 513–516.
- [13] DUAN Yuan-pei, LI Ping. Flow behavior and microstructure evolution of TB8 alloy during hot deformation process [J]. Transaction of Nonferrous Metals Society of China, 2007, 17: 1199–1204.
- [14] LEE W S, LIN M T. The effects of strain rate and temperature on the compressive deformation behavior of Ti-6Al-4V alloy [J]. Mater Processing Technology, 1997, 167: 235–246.
- [15] JONAS J J, SELLSRS C M, McG W J. Strength and structure under hot-working conditions [J]. Int Metal Reviews, 1969, 3(1): 1–24.
- [16] GUAN Shao-kang, WU Li-hong, WANG Li-guo. Flow stress and microstructure evolution of semi-continuous casting AZ70 Mg-alloy during hot compression deformation [J]. Transaction of Nonferrous Metals Society of China, 2008, 18: 315–320.
- [17] BEI Jian-wei, CHEN Wei, XUE Lei, CHENG Shan. Establishment and application of flow stress models of aluminum alloy sheet warm forming [J]. Hot Working Technology, 2009, 38(5): 14–18.

Mg-Y-MM-Zr 合金流变应力模型的建立及应用

马鸣龙¹, 李兴刚¹, 李永军¹, 何兰强¹, 张奎¹, 王献文², 陈丽芳²

1. 北京有色金属研究总院 有色金属材料制备加工国家重点实验室, 北京 100088;

2. 西南铝业股份有限公司, 重庆 401326

摘要: 在 Gleeble-1500D 热模拟机上研究 Mg-9Y-1MM-0.6Zr (WE91)合金的热变形行为, 其变形温度为 653–773 K, 变形速率为 $0.001-1\text{ s}^{-1}$, 变形程度为 60%; 建立 WE91 合金流变应力预测模型。结果表明: 合金的应力和应变之间的关系受变形温度及变形速率的影响, 合金在高温变形过程中的流变应力可以由含 Zener-Hollomon 参数的双曲正弦函数表征, 建立的数学模型可以很好地预测合金的流变应力, 说明该模型可以很好地反映 WE91 合金的变形本质; 合金在真应变为 0.1 时的平均激活能为 220 kJ/mol; 变形温度和变形速率对 WE91 合金的变形组织也有明显的影响。

关键词: 稀土镁合金; Zener-Hollomon 参数; 流变模型; 显微组织

(Edited by LI Xiang-qun)